IET Microwaves, Antennas & Propagation

Research Article

IET Journals
The Institution of Engineering and Technology

Ultra-compact dual-polarised UWB MIMO antenna with meandered feeding lines

ISSN 1751-8725
Received on 4th December 2016
Revised 22nd January 2017
Accepted on 2nd February 2017
E-First on 10th May 2017
doi: 10.1049/iet-map.2016.1074
www.ietdl.org

Muhammad Saeed Khan[1] ✉, Antonio-Daniele Capobianco[1], Adnan Iftikhar[2], Raed M. Shubair[3,4], Dimitris E. Anagnostou[5,6], Benjamin D. Braaten[7]

[1]*Dipartimento di Ingegneria dell'Informazione, University of Padova, Via Gradenigo 6/b, 35131 Padova, Italy*
[2]*Department of Electrical Engineering, COMSATS Institute of IT, Islamabad, Pakistan*
[3]*Electrical and Computer Engineering Department, Khalifa University, Abu Dhabi, UAE*
[4]*Research Laboratory of Electronics, Massachusetts Institute of Technology (MIT), Cambridge, MA, USA*
[5]*Department of Electrical and Computer Engineering, South Dakota School of Mines and Technology, Rapid City, SD 57701, USA*
[6]*Department of Electrical Engineering, Heriot-Watt University, Edinburgh, UK*
[7]*Department of Electrical and Computer Engineering, North Dakota State University, Fargo, ND 58102, USA*
✉ *E-mail: khan@dei.unipd.it*

Abstract: An ultra-compact dual-polarised ultra-wideband multi-input multi-output antenna made with a single-shared-radiating element and two meandered feeding lines are proposed. Miniaturisation is achieved by using a combination of techniques, including a resonant stub connected to the ground through which shorts the excessive coupled energy before it reaches the other port and minimises coupling, slots etched in the radiator that also help minimise mutual coupling, while the meandered lines allow to bring the antenna closer to the greatly reduce the overall size of the antenna. Slots etched in the radiator and the use of a stub connected to the ground through, help to minimise the mutual coupling. The formation of orthogonal surface currents provides the necessary dual polarisation. Simulated and measured results demonstrate the wideband impedance matching, low mutual coupling and low envelope correlation coefficient. This antenna has an extremely compact size (22 × 24.3 mm^2, including the ground plane) that makes it an excellent candidate for portable and handheld devices.

1 Introduction

Ultra-wideband (UWB) technology has been extensively studied in mobile wireless communication systems in recent years, due to its low cost and high data transmission rates. However, conventional UWB technology faces the problem of multipath fading. To mitigate this problem, multi-input multi-output (MIMO) technology has been proposed [1]. MIMO systems have a prominent feature to increase the channel capacity allowing several users to access the various services at the same time. The ultra-wideband technology in combination with MIMO techniques has proved to be an efficient solution for the limitation of short-range communications which require devices to transmit at very low power levels [1].

MIMO antennas require high isolation between the ports. Although the simplest and most effective solution is to keep the distance between multiple antenna elements long, it is incompatible with the miniaturised modern handled and portable devices. Various techniques have been used by designers to achieve high isolation while keeping the antenna size as small as possible [2–12]. Ren *et al.*, for example, achieved high isolation by etching the slots in the radiators and ground plane while reducing the size of the antenna [2]. Liu *et al.* placed a rectangular stub diagonally between two asymmetric coplanar radiators to reduce the mutual coupling [3]. Stubs have also been used on the ground plane between two perpendicularly placed antennas to achieve high isolation along with a compact size antenna in [4]. Stubs and slots were also used together in a co-shared radiator to achieve high isolation in [5]. Another technique involved a floating parasitic digitated decoupling structure which was used on the back side of the radiators to achieve the desired isolation, introduced by Khan *et al.*[6]. A neutralisation line can also be used between antenna elements to reduce the mutual coupling as done in [7]. Other techniques employed a T-shaped reflector in [8], inverted stubs . in [9], different elements for polarisation diversity in [10] and a perpendicular feeding network in [11]. In [13], different methods are explained to design the meander line antenna; however, the focus is on the antenna element, not on the transmission line. In [14], two meander line antennas using metamaterial concept are designed. In all aforementioned designs, there is always a trade-off between the bandwidth, size and complexity.

This paper presents an extremely compact dual-polarised UWB-MIMO antenna (shown in Fig. 1) that consists of a single ultra-wideband monopole fed by two perpendicular meandered microstrip lines. With this configuration, a strong reduction of the size with respect to all existing designs is achieved. To reduce the unavoidable mutual coupling, slots are etched on the radiator with the addition of an open shunt stub placed at the centre of the structure. Placing the open stub on the antenna and feeding the antenna with modified microstrip lines are used for the first time in a UWB-MIMO antenna and also connecting the stub to the ground through provides the current a path to the stub. The proposed antenna has an ultra-compact size (22 × 24.3 mm^2), which is 35% smaller than the design presented in [3], and is one of the smallest currently available in the literature. The simulated and measured results showed that the proposed antenna has a wideband impedance matching, low mutual coupling and low envelope correlation coefficient (ECC), which makes it suitable for portable handheld devices.

2 Antenna design

The steps to finalise the proposed MIMO antenna are shown in Fig. 2. As a starting point, a rectangular monopole was designed with a partial ground plane. This monopole was then fed by two straight perpendicular 50 Ω microstrip lines that were connected to the arched portion of the radiator that improve the matching bandwidth, as shown in Fig. 2*a* (black solid line). A wideband matching was observed (shown in Fig. 3), but the isolation was low (shown in Fig. 4). Specifically, both ports are well matched ($|S_{11}| <$

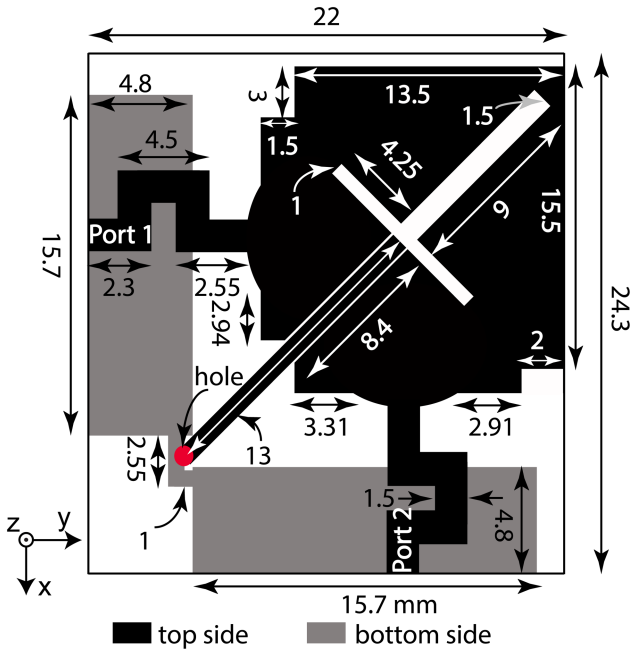

Fig. 1 *Geometry of the proposed UWB-MIMO antenna system. All dimensions are in mm*

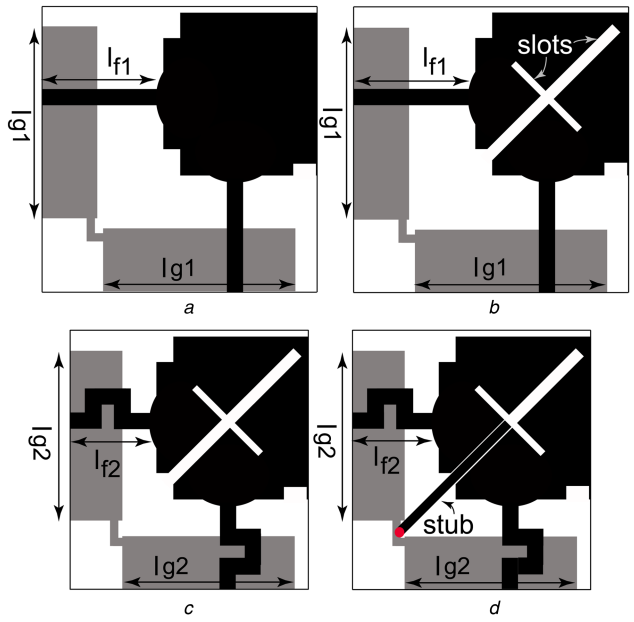

Fig. 2 *Steps involved during the design procedure*
(a) Without slots, ***(b)*** With slots, ***(c)*** With folded transmission lines and slots, ***(d)*** With folded transmission lines, slots and stub (final design)

−10 dB and $|S_{22}| < -10$ dB) from 3 to 11 GHz, as shown in Figs. 3*a* and *b*, but the mutual coupling $|S_{12}|$ or $|S_{21}|$ was high from 3 to 7 GHz, as shown in Fig. 4. To reduce mutual coupling between the two feeding ports, slots were etched on the radiator (Fig. 2*b*). These slots force the RF current to concentrate on the edges of the structure (Fig. 5*a*), instead of travelling directly from one port to the other, and help reduce mutual coupling [5], by >50%. As expected, there was very little effect of these slots on the impedance bandwidth, as shown in Figs. 3*a* and *b*.

To further reduce the size of the antenna, the microstrip lines were meandered as shown in Fig. 2*c*, the total distance from the port and antenna feed was reduced from $l_{f1} = 9.35$ mm to $l_{f2} = 6.35$ mm, but the electrical length of the microstrip lines was maintained. This technique was necessary since the reduced size of the ground prevents to simply shorten the straight microstrips without affecting their line impedance. Nevertheless, a slight mismatch was still present: a fine tuning procedure was

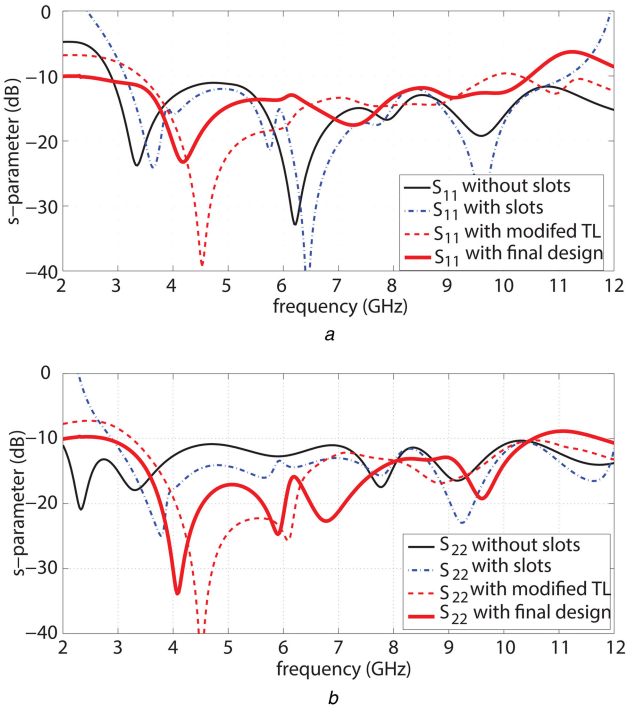

Fig. 3 *Simulated S-parameters of antenna with slots, without slots, with modified feed line and stub*
(a) S_{11}, ***(b)*** S_{22}

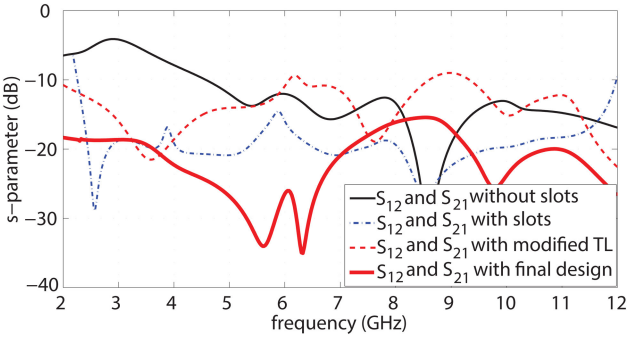

Fig. 4 *Simulated mutual coupling of antenna with slots, without slots, with modified feed line and stub*

implemented acting also on the size of the partial ground reducing its size from $l_{g1} = 18.5$ mm to $l_{g2} = 15.7$ mm. The bends of the meandered microstrip sections ultimately increase energy leakage and thus the mutual coupling. A $\lambda/4$ (at 5.5 GHz) open-circuit stub that is 13 mm long was then placed between the elements. The stub is shorted to the ground on one end and resonates at 5.5 GHz (as shown in Fig. 4). This resonance helps short to the ground the leaked energy and thus increases the isolation and reduces the coupling between the two ports from about 4.5 to 7 GHz. Its function is similar to that of a band-stop filter having through inductance (series inductance) and shunt capacitance, hence reducing the mutual coupling. The open-circuit stub is connected to the ground using as shown in Fig. 2*d*.

To illustrate the effectiveness of the slots and the stub, the simulated surface current distribution with and without the stub is shown in Fig. 5. When there is no stub, the current is concentrated on the slot edges, but the current is also travelling to Port 2 (as shown in Fig. 5*a*), which results in high coupling at 5.5 GHz. When the stub is added and attached to the ground plane using the conducting via, the current finds an additional path to travel, as shown in Fig. 5*b*, the current which was travelling to the other side of the ground is now concentrated on the stub. The dual-polarised behaviour can be explained by observing the flow of the simulated currents on the surface of the antenna in Fig. 6. When Port 1 is excited, the current flows mainly in the *y*-direction along the radiator, as depicted in Fig. 6*a*, and exists mostly on the left side of

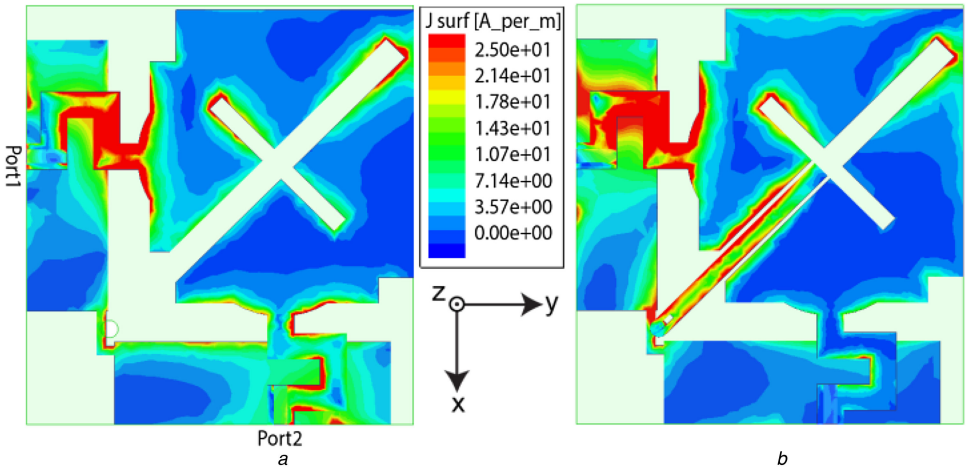

Fig. 5 *Simulated surface current distribution at 5.5 GHz while feeding only Port 1*
(a) Without stub, ***(b)*** With stub. When the stub is connected, the current finds an extra path, hence the reduced mutual coupling

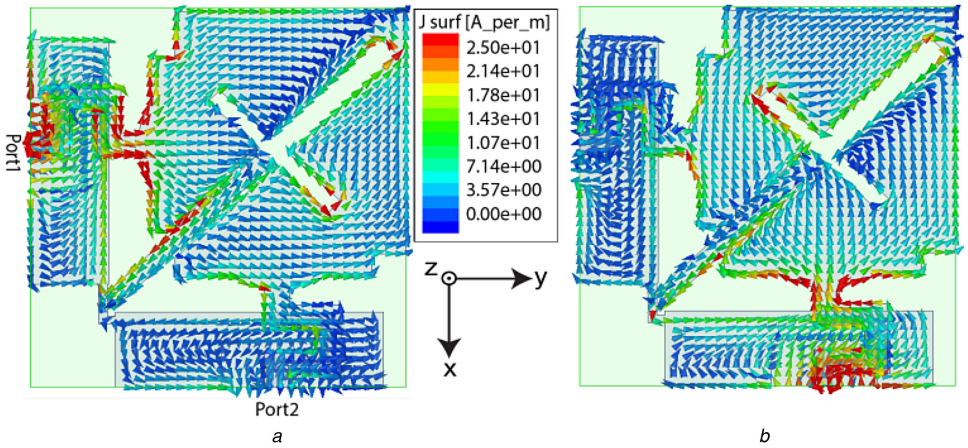

Fig. 6 *Simulated surface current distribution at 6.5 GHz*
(a) Port 1 was excited, ***(b)*** Port 2 was excited

Table 1 Performance comparison with previous published literature

Published literature	Total occupied size, mm^2	Bandwidth, GHz	Isolation, dB	Gain var-(dBi)/ total efficiency, %	ECC using far-field patterns
[6]	1501.5	3.1–10.6	>15	**2.3/85**	<0.6
[2]	1024	3.1–10.6	>15	2.5/60	NA
[3]	812.25	2.66–10.8	>15	2.2/NA	NA
[10]	1400	3.0–10.6	>15	3.1/NA	NA
proposed antenna	**534.6**	**3–10.6**	>15	4/82	**<0.42**

In each column, the dominant feature of the antenna when compared to all others is highlighted in bold. The proposed antenna has more dominant features than other antennas.

the antenna. Any coupled current on the right side of the antenna flows mostly in the *x*-direction, and is significantly lower in amplitude, as shown in Fig. 6*a*. Similarly when Port 2 is excited, the current on the right side mainly flows in the *x*- direction and the coupled current on the left side (that is smaller in amplitude) of the antenna, flows in the *y*-direction, as depicted in Fig. 6*b*. Due to these orthogonal currents on the elements, the dual-polarised characteristics were attained in the far-field.

In Table 1, the proposed antenna is compared with the most representative UWB-MIMO antennas presented in the literature. The list is not comprehensive but fairly represents the current state of the art of this technology. Table 1 shows that the proposed design is compact having almost same of better features.

3 Results and discussion

3.1 S-parameters

The proposed antenna was fabricated on a Rogers TMM4 60 mil thick substrate with dielectric permittivity 4.5 and loss tangent 0.002. The prototype is shown in Fig. 7. The measurements were taken using an Agilent E5071C network analyser. The simulated and measured scattering parameters are plotted in Fig. 8 and very good agreement between simulated and measured results was observed. Although the design looks symmetric in shape along Ports 1 and 2, its dimensions are not exactly the same along the ports and this cause the $|S_{11}|$ response to differ from the $|S_{22}|$ response. The measurements satisfy the UWB-MIMO requirement from 3.2 to 10.6 GHz (i.e. $|S_{11,\,22}| < -10$ dB, and $|S_{12,\,21}| < -15$ dB [4–6]).

3.2 Radiation patterns and gain

The measured and simulated radiation patterns can be compared in Fig. 9. The simulated and measured radiation patterns showed good agreement. For the pattern measurements, a coaxial cable with ferrite beads was used to reduce the return currents and cable effects. When Port 1 is excited, the θ-component is dominant in the *yz*-plane and the φ-component is dominant in the *xz*-plane. The θ-component of the electric field in the *yz*-plane has a toroidal shape

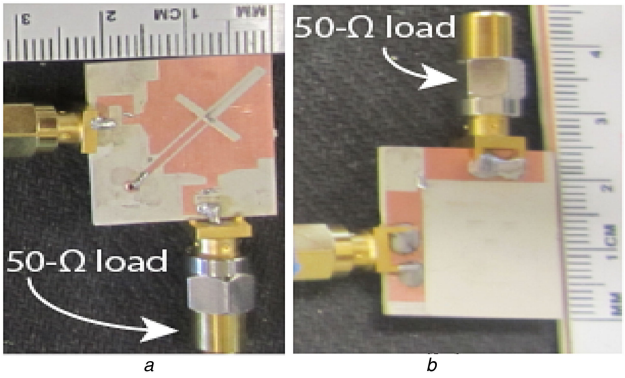

Fig. 7 *Photograph of printed prototype with short feeding cable used in measurement*
(a) Top side, ***(b)*** Bottom side

at lower frequencies. As the frequency increases, the patterns deviate slightly from this shape, as expected from the changed current distribution. In the *xz*-plane, the φ-component has omnidirectional patterns at the lower frequencies that become less omnidirectional at higher frequencies. Similarly for Port 2, the φ-component is dominant in the *yz*-plane and the θ-component is dominant in the *xz*-plane. Similar behaviour of the patterns is observed for Port 2 in the perpendicular planes.

The measured gain of the antenna is shown in Fig. 10, and is very close to the simulated one. The gain increases almost linearly from 1.8 to 5.8 dBi throughout the UWB band. The measured efficiency (shown in Fig. 11) matched the simulated efficiency when the simulation included the cable model. A good agreement with the measured results was observed, noting that the measured efficiency of the antenna with the cable connected was less than the simulated without cable (>82%), particularly at the lower frequencies. This was undoubtedly due to cable losses, substrate losses and mismatching.

3.3 Diversity analysis

The diversity performance of an MIMO system can be verified on the basis of the ECC [15]. The ECC can be computed by using scattering parameters or far-field radiation patterns. The computed value of the ECC from the *S*-parameters, according to [15], was found to be <0.01, while when it was calculated from the far-field patterns as presented in [16], the values were found to be <0.42 for isotropic, indoor and outdoor environments. The ECC value of <0.7 is considered to be suitable for diversity applications [10, 17].

4 Effects of large ground plane on the proposed antenna

It is true that such MIMO antennas must often be connected onto a larger ground plane. Although the specifics of each design are things that the design engineers can address and optimise on a case-by-case basis (especially for commercial applications), the simulations of the proposed antenna with large ground planes of variable size validate the usefulness of the design as they show that

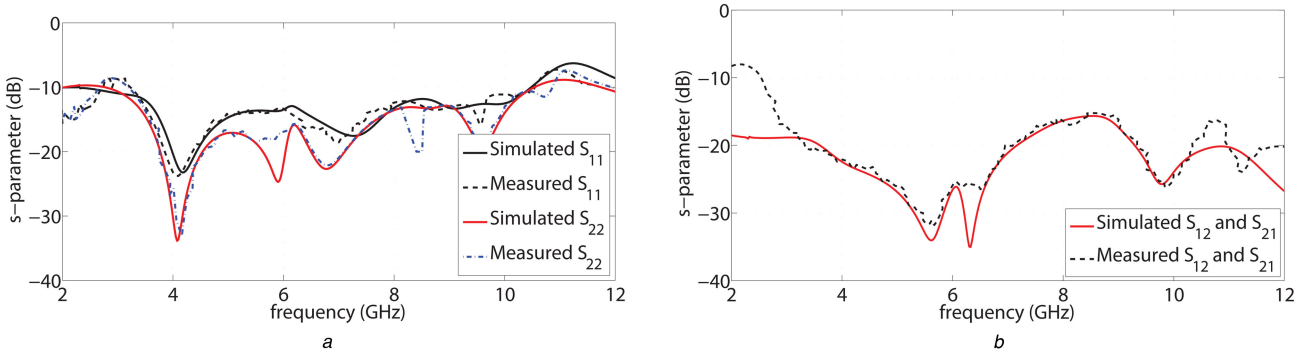

Fig. 8 *Simulated and measured S-parameters of antenna*
(a) S_{11} and S_{22}, ***(b)*** S_{12} or S_{21}

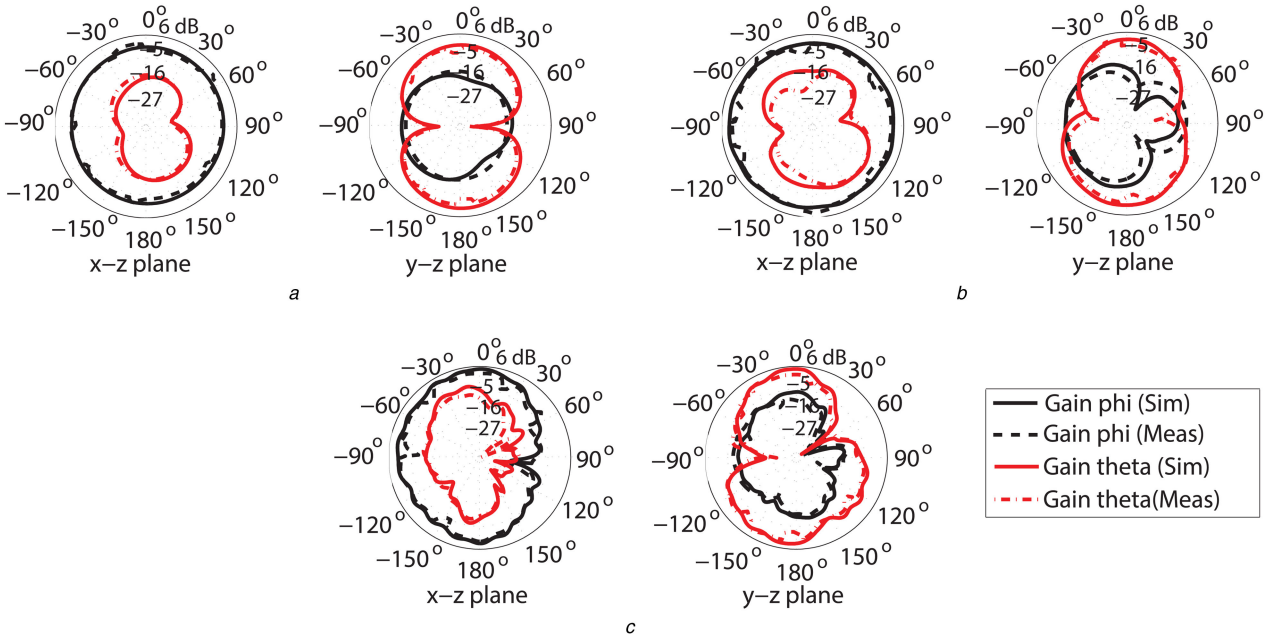

Fig. 9 *Simulated and measured radiation patterns while only Port 1 was excited*
(a) 3.5 GHz, ***(b)*** 6.5 GHz, ***(c)*** 9.5 GHz

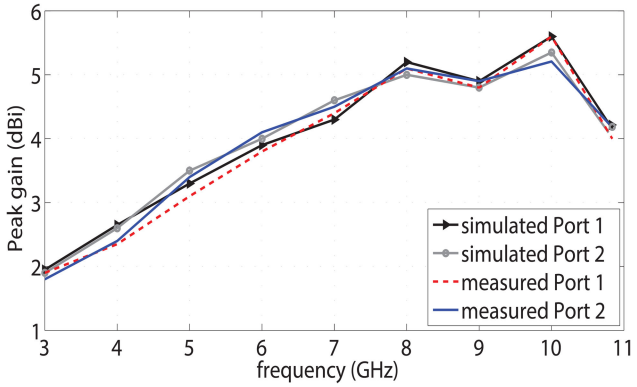

Fig. 10 *Simulated and measured peak gain showing a variation of 4 dBi*

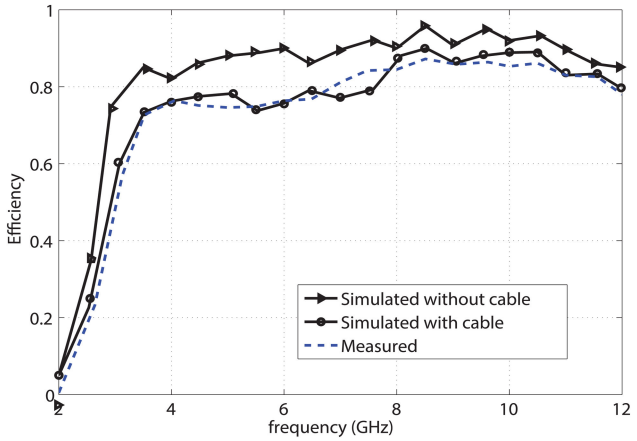

Fig. 11 *Simulated and measured efficiency*

the antenna can easily be attached on larger platforms with smartphone-like dimensions.

To study the effects of large ground plane on the proposed antenna, a large ground plane was connected to the ground plane of the proposed antenna in the simulation through 1×1 mm^2 strip as shown in Fig. 12. The small strip was used to enable an electrical connection while minimising the effect of the large ground plane, as it can be observed. The results in Fig. 13 show that the large ground plane affected the S-parameters very little but the requirements of UWB-MIMO are still fulfilled, i.e. $S_{11} < -10$ dB and $S_{21} < -15$ dB. The length of the large ground plane was varied from $L = 100$ to 140 mm and width was varied from $W = 45$ to 65 mm. The large ground plane affected the higher band much more than the middle and lower band of the proposed antenna. These

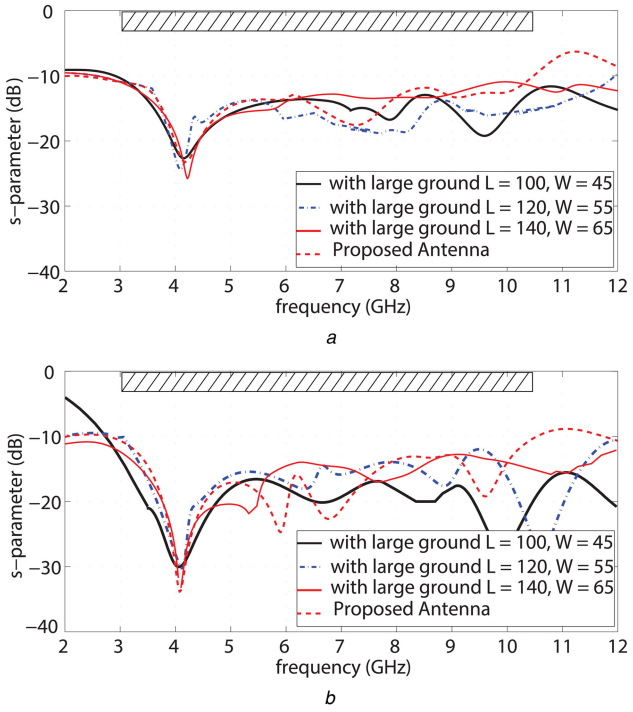

Fig. 13 *Effects of large ground plane on* ***(a)*** S_{11}, ***(b)*** S_{22}

results show the effectiveness of the proposed antenna for portable devices.

5 Conclusion

An ultra-compact dual-polarised UWB-MIMO antenna with a single, shared radiator was proposed. The radiator's feed that consisted of folded microstrip lines, along with a combination of miniaturisation and coupling reduction techniques allowed for an ultra-compact structure, arguably the smallest available in the current literature. Miniaturisation with low mutual coupling was achieved by introducing slots on the radiator, and a shorted stub between the two elements. The antenna dual polarisation capabilities, along with the low mutual coupling between the two ports, low ECC, extremely compact size (22×24.3 mm^2), omnidirectional radiation patterns and wide bandwidth (covering the 3.1–10.6 GHz range), make the proposed ultra-compact UWB-MIMO antenna an excellent candidate for portable handheld and mobile devices.

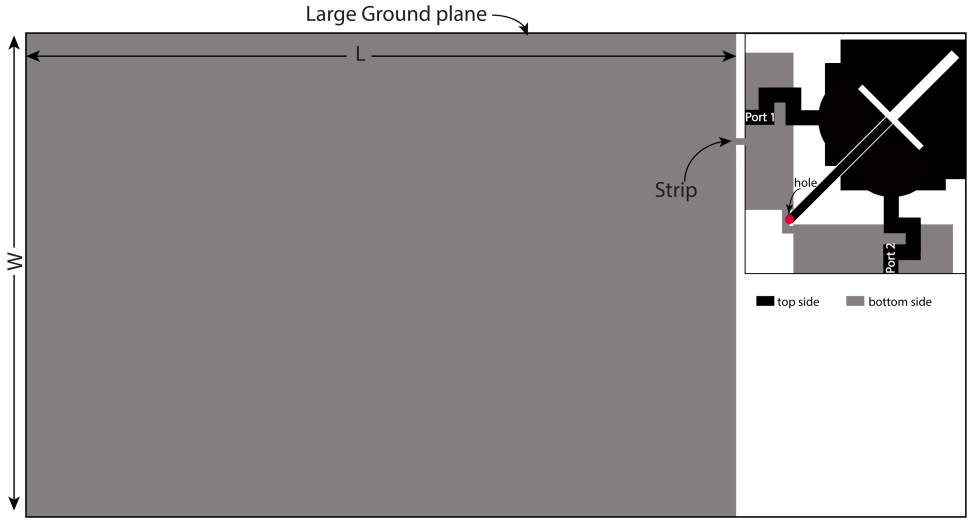

Fig. 12 *The proposed antenna connected with a large ground plane through 1 × 1 mm^2 strip*

6 Acknowledgment

The authors acknowledge financial support from the University of Padova, project CPDA150022.

7 References

[1] See, T.S.P., Chen, Z.N.: 'An ultra-wideband diversity antenna', *IEEE Trans. Antennas Propag.*, 2009, **57**, (9), pp. 1597–1605

[2] Ren, J., Hu, W., Yin, Y.*, et al.*: 'Compact printed MIMO antenna for UWB applications', *IEEE Antenna Wirel. Propag. Lett.*, 2014, **13**, pp. 1517–1520

[3] Liu, Y.F., Wand, P., Qin, H.: 'Compact ACS-fed UWB antenna for diversity applications', *IET Electron. Lett.*, 2014, **50**, (19), pp. 1336–1338

[4] Liu, L., Cheung, S.W., Yuk, T.I.: 'Compact MIMO antenna for portable devices in UWB applications', *IEEE Trans. Antennas Propag.*, 2013, **61**, (8), pp. 4257–4264

[5] Mao, C.X., Xhu, Q.X.: 'Compact coradiator UWB-MIMO antenna with dual polarization', *IEEE Trans. Antennas Propag.*, 2014, **62**, (9), pp. 4474–4480

[6] Khan, M.S., Capobianco, A.D., Najam, A.I.*, et al.*: 'Compact ultra-wideband diversity antenna with a floating parasitic digitated decoupling structure', *IET Microw. Antenna Propag.*, 2014, **8**, (10), pp. 747–753

[7] Su, S.W., Lee, C.T., Chang, F.S.: 'Printed MIMO-antenna system using neutralization-line technique for wireless USB-dongle applications', *IEEE Trans. Antennas Propag.*, 2012, **60**, (2), pp. 456–463

[8] Capobianco, A.D., Khan, M.S., Caruso, M.*, et al.*: '3–18 GHz compact planar antenna for short-range radar imaging', *IET Electron. Lett.*, 2014, **50**, (14), pp. 1016–1018

[9] Khan, M.S., Shafique, M.F., Capobianco, A.D.*, et al.*: 'Compact UWB-MIMO antenna array with a novel decoupling structure'. Proc. of 10th Int. Bhurban Conf. on Applied Sciences and Technology, January 2013, pp. 347–350

[10] Zhang, S., Lau, B.K., Sunesson, A.*, et al.*: 'Closely-packed UWB MIMO/diversity antenna with different patterns and polarizations for USB dongle applications', *IEEE Trans. Antennas Propag.*, 2012, **60**, (9), pp. 4372–4380

[11] Adamiuk, G., Beer, S., Wiesbeck, W.*, et al.*: 'Dual-orthogonal polarized antenna for UWB-IR technology', *IEEE Antennas Wirel. Propag. Lett.*, 2009, **8**, pp. 981–984

[12] Khan, M.S., Capobianco, A.-D., Iftikhar, A.*, et al.*: 'A compact dual polarized ultrawideband multiple-input multiple-output antenna', *Microw. Opt. Technol. Lett.*, 2016, **58**, (1), pp. 163–166

[13] Jahanbakhshi, A., Moradi, Gh.: 'Design and simulation of different types of meander line antennas with improved efficiency'. PIERS Proc., Russia, August 2012, pp. 594–597

[14] Ryan, C.G.M., Eleftheriades, G.V.: 'Two compact, wideband, and decoupled meander-line antennas based on metamaterial concepts', *IEEE Antennas Wirel. Propag. Lett.*, 2012, **11**, pp. 1277–1280

[15] Balanch, S., Romeu, J., Corbella, I.: 'Exact representation of antenna system diversity performance from input parameter description', *Electron. Lett.*, 2003, **39**, (9), pp. 705–707

[16] Knudsen, M.B., Pedersen, G.F.: 'Spherical outdoor to indoor power spectrum model at the mobile terminal', *IEEE J. Sel. Areas Commun.*, 2002, **20**, (6), pp. 1156–1168

[17] Vaughan, R.G., Anderson, J.B.: 'Antenna diversity in mobile communications', *IEEE Trans. Veh. Technol*, 1987, **36**, (4), pp. 149–172